Acyl Chain-Length Asymmetry Alters the Interfacial Elastic Interactions of Phosphatidylcholines

Shaukat Ali, Janice M. Smaby, Maureen M. Momsen, Howard L. Brockman, and Rhoderick E. Brown
The Hormel Institute, University of Minnesota, Austin, Minnesota 55912 USA

ABSTRACT Phosphatidylcholines (PCs) with stearoyl (18:0) *sn*-1 chains and variable-length, saturated *sn*-2 acyl chains were synthesized and investigated using a Langmuir-type film balance. Surface pressure was monitored as a function of lipid molecular area at various constant temperatures between 10°C and 30°C. Over this temperature range, 18:0–10:0 PC displayed only liquid-expanded behavior. In contrast, di-14:0 PC displayed liquid-expanded behavior at 24°C and 30°C, but two-dimensional phase transitions were evident at 20°C, 15°C, and 10°C. The average molecular area of 18:0–10:0 PC was larger than that of liquid-expanded di-14:0 PC at equivalent surface pressures, and the shapes of their liquid expanded isotherms were somewhat dissimilar. Analysis of the elastic moduli of area compressibility (C_s^{-1}) as a function of molecular area revealed shallower slopes in the semilog plots of 18:0–10:0 PC compared to di-14:0 PC. At membrane-like surface pressures (e.g., 30 mN/m), 18:0–10:0 PC was 20–25% more elastic (in an in-plane sense) than di-14:0 PC. Other PCs with varying degrees of chain-length asymmetry (18:0–8:0 PC, 18:0–12:0 PC, 18:0–14:0 PC, 18:0–16:0 PC) were also investigated to determine whether the higher in-plane elasticity of fluid-phase 18:0–10:0 PC is a common feature of PCs with asymmetrical chain lengths. Two-dimensional phase transitions in 18:0–14:0 PC and 18:0–16:0 PC prevented meaningful comparison with other fluid-phase PCs at 30 mN/m. However, the C_s^{-1} values for fluid-phase 18:0–8:0 PC and 18:0–12:0 PC were similar to that of 18:0–10:0 PC (85–90 mN/m). These values showed chain-length asymmetrical PCs to have 20–25% greater in-plane elasticity than fluid-phase PCs with mono- or diunsaturated acyl chains.

INTRODUCTION

Physical studies of phosphatidylcholines (PCs) have provided important insights into fundamental processes that occur within lipid bilayers. For instance, investigations of PCs in which the *sn*-1 and *sn*-2 acyl chains differ markedly in length have provided the bulk of current knowledge regarding transbilayer acyl chain interdigitation of lipids (for reviews, see Huang and Mason, 1986; Slater and Huang, 1988, 1992). Yet often overlooked is the fact that PCs containing highly asymmetrical chain lengths can be physiologically important in situations where their ability to interdigitate may be of secondary importance. In studies of yeast grown under anaerobic conditions in the presence of stearolate or hydroxystearate but in the absence of oleate (or other olefinic fatty acids), Meyer and Bloch (1963) noted a decrease in the unsaturated fatty acyl content of PC. The decrease was compensated by the appearance of short saturated acyl chains (10:0, 12:0, and 14:0) that localized exclusively to the *sn*-2 position of PC. Later, Proudlock et al. (1971) showed that yeast mutants lacking the capacity to synthesize 16- or 18-carbon unsaturated fatty acids increased their levels of short-chain, saturated fatty acids when subjected to growth conditions of unsaturated fatty acid restriction. The increase in short-chain, saturated fatty acids was evident under aerobic conditions, but was clearly exacerbated by anaerobisis. Exactly how well short-chain, saturated fatty acyl chains in the *sn*-2 position of phospholipids are able to mimic the liquid-crystalline phase features produced by their longer unsaturated counterparts is not well understood.

Indeed, most physical studies involving PCs with highly asymmetrical length, saturated chains have focused on the gel-phase bilayer properties because of the static interdigitation of acyl chains that occurs (e.g., Huang, 1990). Compared to their symmetrical chain-length counterparts, PCs with asymmetrical length chains can form thinner bilayers (Hui et al., 1984; McIntosh et al., 1984), especially in cases of mixed and fully interdigitated lipids. Having a thinner, interdigitated gel phase coexisting with a liquid-crystalline phase is postulated to enhance the formation and/or stabilization of lipid domains in biological membranes (e.g., Schram and Thompson, 1995). In the case of the liquid-crystalline properties of lipids with asymmetrical length acyl chains, less is known. From Fourier transform infrared, ^{2}H-NMR, fluorescence, and diffraction studies of liquid-crystalline PCs with highly asymmetrical chain lengths, a partial transbilayer interdigitation of a dynamic, "statistical" nature is thought to occur, with the longer acyl chains rapidly sampling both their own as well as the apposing monolayer (Lewis et al., 1994; Mason, 1994; Zhu and Caffrey, 1993). The impact of this dynamic, "statistical" interdigitation on the ensemble of liquid-crystalline, physi-

Received for publication 28 July 1997 and in final form 14 October 1997.

Address reprint requests to Dr. Rhoderick E. Brown, Hormel Institute, 801 16th Ave. NE, Austin, MN 55912. Tel.: 507-433-8804; Fax: 507-437-9606; E-mail: reb@maroon.tc.umn.edu.

Dr. Ali's present address is The Liposome Company, One Research Way, Princeton, NJ 08540-6619. E-mail: sali@lipo.com.

Portions of this investigation were presented at the 40th Annual Meeting of the Biophysical Society held in Baltimore, Maryland (Ali et al., 1996) and at the FASEB Summer Conference on Molecular Biophysics of Cellular Membranes held at Saxton's River, Vermont, on July 20–25, 1996.

0006-3495/98/01/338/11 $2.00

cal properties appears to be somewhat paradoxical and is not well understood. For instance, NMR and fluorescence evidence suggests that the conformational order of the acyl chains in liquid-crystalline, asymmetrical-chain PCs differs from that of symmetrical-chain PCs (Halladay et al., 1990; Lewis et al., 1994; Mason, 1994). Yet the translational diffusion of *N*-7-nitrobenz-2-oxa-1,3-diazol-4-yl-amino (NBD)-labeled PE reportedly is the same in either 18:0–10:0 PC or in di-14:0 PC liquid crystalline bilayers (Schram and Thompson, 1995). Hence the expected frictional drag along the midplane within bilayers experiencing "statistical" interdigitation is either insufficient to affect lipid translational diffusion rates in liquid-crystalline bilayers or is compensated by other properties of the asymmetrical-chain lipids. One such compensatory property might be subtle changes in the lipid-lipid interactions to produce a fluid packing state in which the in-plane elasticity is somewhat higher when the lipids have hydrocarbon chains of asymmetrical length compared to when the acyl chains are similar in length.

Here we establish the nature of the interfacial elastic interactions that occur among asymmetrical-chain PCs under conditions where no acyl chain interdigitation is possible by using Langmuir film balance approaches to investigate a series of PCs in which the *sn*-1 chain is stearate (18:0) and the *sn*-2 chain is varied (8:0, 10:0, 12:0, 14:0, 16:0, or 18:0). Recently we demonstrated how this approach provides insights into the interfacial elastic packing interactions of PCs (with approximately symmetrical-length chains) (Smaby et al., 1996), as well as how cholesterol-induced decreases in the in-plane elasticity of PCs are regulated by the level and position of *cis* double bonds in the acyl chains (Smaby et al., 1997). Here we show that PCs with marked chain-length asymmetry (e.g., 18:0–8:0 PC or 18:0–10:0 PC) display 20–25% greater in-plane elasticity than PCs with more symmetrical-length acyl chains (e.g., 16:0–18:1$^{\Delta 9(c)}$ PC or di18:1$^{\Delta 9(c)}$ PC) at surface pressures approximating membrane conditions.

MATERIALS AND METHODS

Lipid synthesis

Distearoyl phosphatidylcholine (PC) and 1-stearoyl-lyso PC were purchased from Avanti Polar Lipids (Alabaster, AL), and fatty acid anhydrides were obtained from Nu-Chek Prep (Elysian, MN). All other PCs were synthesized by reacting 1-stearoyl-lyso PC with the desired fatty acid anhydride (8:0, 10:0, 12:0, 14:0, or 16:0) in the presence of the catalyst 4-pyrrolidinopyridine, as described previously (Ali and Bittman, 1989). The resulting PCs were purified by flash column chromatography, using step-gradient solvent mixtures consisting of $CHCl_3$, $CHCl_3/CH_3OH$ (9:1) and $CHCl_3/CH_3OH$ (1:1) in sequential fashion. Final purification was achieved by preparative thin-layer chromatography (TLC) with 1-mm plates (Analtech, Newark, DE) with $CHCl_3/CH_3OH/H_2O$ (60:30:5). Silica gel "fines" were removed from the PCs with Metricel syringe filters (0.2 μm; Gelman Sciences, Ann Arbor, MI). Final lipid purity was greater than 99%, based on TLC ($CHCl_3/CH_3OH/H_2O$, 60:30:5).

Monolayer conditions

Stock solutions of PCs were prepared by dissolving lipids in either petroleum ether/ethanol or hexane (Burdick Jackson Laboratories, Muskegon, MI)/ethanol (95:5). Solvent purity was verified by dipole potential measurements (Smaby and Brockman, 1991a). PCs were assayed quantitatively based on phosphate concentration (Bartlett, 1959). Water for the subphase buffer was purified by reverse osmosis, activated charcoal adsorption, and mixed-bed deionization; then passed through a Milli-Q UV Plus System (Millipore Corp., Bedford, MA); and filtered through a 0.22-μm Millipak 40 membrane. Subphase buffer (pH 6.6) consisting of 10 mM potassium phosphate, 100 mM NaCl, and 0.2% NaN_3 was stored under argon until use.

Surface pressure-molecular area-surface potential (π-A) isotherms were measured under a humidified argon atmosphere with a computer-controlled, Langmuir-type film balance, calibrated according to the equilibrium spreading pressures of known lipid standards (Momsen et al., 1990), and housed in a laboratory with a filtered air supply. Lipids were dissolved (51.67-μl aliquots) and spread in hexane/ethanol (95:5). Films were compressed at a rate of $\leq$4 Å^2/molecule/min after an initial delay period of 4 min. The subphase was maintained at fixed temperature with a thermostatted, circulating water bath. Dipole potentials were measured with a ^{210}Po ionizing electrode.

Analysis of isotherms

Monolayer phase transitions were identified from the second and third derivatives of surface pressure (π) with respect to molecular area (A) as previously described (Ali et al., 1991). Monolayer compressibilities at the indicated experimental mixing ratios were obtained from π-A data, using

$$C_s = (-1/A)(dA/d\pi) \quad (1)$$

where A is the area per molecule at the indicated surface pressure and π is the corresponding surface pressure (e.g. Behroozi, 1996). For convenience, we expressed the data in terms of the reciprocal of isothermal compressibility (C_s^{-1}), i.e., surface compressional moduli (Davies and Rideal, 1963), because this facilitated comparisons with bulk elastic moduli of area compressibility measurements made in bilayer systems (e.g., Evans and Needham, 1987; Needham and Nunn, 1990). We used a 100-point sliding window that utilized every fourth point to calculate a C_s^{-1} value before advancing the window one point. Each C_s^{-1} versus average molecular area curve consisted of 200 C_s^{-1} values obtained at equally spaced molecular areas along the π-A isotherms.

In recent reports in which the π-C_s^{-1} behaviors of various pure GalCers, SMs, and PCs as well as PC-cholesterol mixtures were investigated (Smaby et al., 1996, 1997), we discussed the limitations associated with experimentally derived C_s^{-1} values obtained at high surface pressures (>30–35 mN/m). In essence, C_s^{-1} values determined directly from an experimental π-A isotherm display a maximum below collapse and then diminish at higher surface pressures instead of hyperbolically increasing until film collapse. The C_s^{-1} maximum generally occurs at surface pressures greater than 35 mN/m, but this depends somewhat upon the lipid or lipid mixture under study. Actually, C_s^{-1} values begin to fall away from the expected hyperbolic-like increase before achieving the C_s^{-1} maximum (Fig. 1 *B*). The highly reproducible C_s^{-1} maximum may indicate a precollapse behavior that is linked to intrinsic experimental factors (e.g., trough composition and/or design), but may also reflect a decrease in lipid film stability at high pressures (e.g., Schwarz et al., 1996). Analogously, the dipole potential (ΔV) versus inverse area behavior ($1/A$) of various liquid-expanded lipids reportedly is linear up to surface pressures where the second derivative of the π-A isotherms ($d^2\pi/dA^2$) goes from positive to negative values (π_d) (Smaby and Brockman, 1990). The linearity indicates a lack of significant dipole reorientation over the range of surface pressures leading up to π_d, and typically encompasses 80–90% of the π-A data for liquid-expanded films. Hence to improve the C_s^{-1} data at high surface pressures, we fit the experimentally obtained π-A isotherms to the follow-

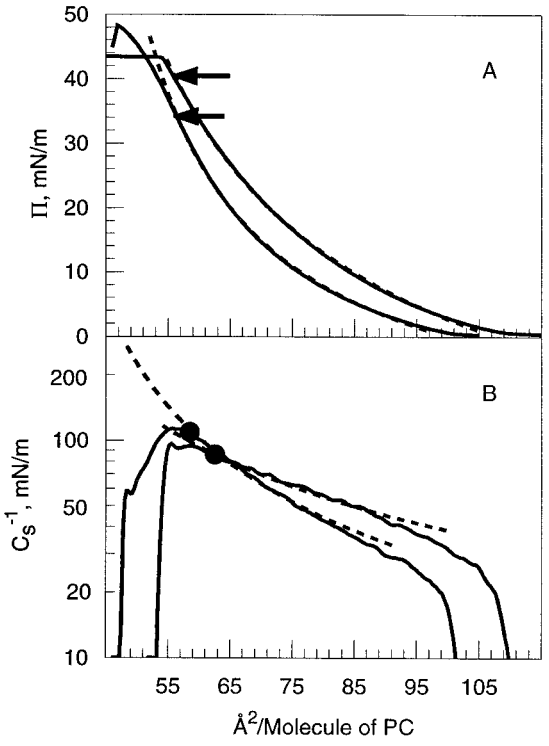

FIGURE 1 Comparison of 18:0–10:0 PC and di-14:0 PC monolayers. (*A*) Surface pressure versus average cross-sectional molecular area (π-A). Experimentally observed isotherms at 24°C are represented by the solid lines. The left-hand isotherm pair is di-14:0 PC, and the right-hand isotherm pair is 18:0–10:0 PC. Arrows indicate where $d^2\pi/dA^2$ goes from positive to negative. The fitted isotherms (– – –) were generated from the experimental isotherms, using Eq. 2 as described in Materials and Methods. (*B*) Interfacial elastic modulus of area compressibility (C_s^{-1}) versus average molecular area. C_s^{-1} values were calculated from the experimentally observed π-A isotherms in *A*, using the inverse of Eq. 1 as described in Materials and Methods (——). The maximum C_s^{-1} value occurs where $d^2\pi/dA^2$ goes from positive to negative on the corresponding π-A isotherm in *A*. The symbol on each curve indicates a surface pressure of 30 mN/m. C_s^{-1} values calculated from the fitted π-A isotherms in *A* (using the inverse of Eq. 1) are shown as dashed lines in *B*. Each dashed line in *B* covers the surface pressure range of 3 mN/m to film collapse.

ing osmotic-based monolayer equation of state:

$$\pi = (qkT/\omega_1)\ln[(1/f_1)[1 + \omega_1/(A_\pi - \omega_0)]] \qquad (2)$$

where k is Boltzmann's constant, ω_1 is the cross-sectional area of an interfacial water molecule (9.65 Å^2), ω_0 is the cross-sectional area of dehydrated lipid, f_1 is the activity coefficient of interfacial water, and A_π is the total surface area divided by the number of lipid molecules present at a given surface pressure (Wolfe and Brockman, 1988; Smaby and Brockman, 1992; Feng et al., 1994). The scaling parameter q correlates to f_1 and is not unique, but does provide a better fit of the data because it allows for higher order terms involving the activity coefficient (Smaby and Brockman, 1991b; Feng et al., 1994). Because data obtained near the high- and low-pressure limits often are especially sensitive to the dynamics of the experiment and to trace impurities, respectively (e.g., Middleton and Pethica, 1981), the upper limit for reliable π-A data was defined as the value at which $d^2\pi/dA^2$ goes from positive to negative (typically 10–15% below film collapse), and the lower limit was determined by the molecular area where $\pi = 1.0$ mN/m. From the regions of the π-A experimental data satisfying the preceding criteria, fitted π-A isotherms were generated that provided extrapolated π-A data at high π (approaching film collapse). C_s^{-1} values could then be determined from the extrapolated high-pressure data ($\pi \geq 30$ mN/m).

Fig. 1 *A* illustrates the quality of the curve fitting for pure 18:0–10:0 PC compared with di-14:0 PC at 24°C. The dashed lines show the fitted isotherms resulting when the experimental π-A isotherms (*solid lines*) are fit using Eq. 2. The arrow positioned along each experimental π-A isotherm indicates where $d^2\pi/dA^2$ changes from positive to negative. This change occurs at the same mean molecular area where the C_s^{-1} maximum is observed in the experimentally derived C_s^{-1} versus average area plot (Fig. 1 *B*, *solid lines*). The dashed lines in Fig. 1 *B* correspond to the C_s^{-1} versus average area behavior calculated from the fitted π-A isotherms, using the inverse of Eq. 1. The symbols designate the surface pressure of 30 mN/m along each curve in Fig. 1 *B*. How closely the extrapolated C_s^{-1} values match their experimental counterparts depends on both PC acyl structure and the two-dimensional phase state (Smaby et al., 1997). When the lipids are liquid-expanded at 30 mN/m, the correspondence is good but diminishes at higher surface pressures (see Table 1; Exptl. C_s^{-1} versus Fitted C_s^{-1}). Because the osmotic-based monolayer equation of state (Eq. 2) used to fit the data has been shown to be most reliable for liquid-expanded behavior (Smaby and Brockman, 1991b; Feng et al., 1994), we limited the application of the fitting procedure to the liquid-expanded isotherms (Table 1). The important point is that, regardless of whether one uses the experimental values or the fitted values at 30 mN/m, remarkably similar trends are observed in the way that acyl chain-length asymmetry affects the different PC molecular species, and the experimental and fitted C_s^{-1} values differ only slightly (Table 1). All data in Figs. 2-10 represent experimental data and C_s^{-1} values generated directly from the data without fitting to Eq. 2.

Calculation of the chain-length inequivalence and overall nonpolar chain length of PCs

To calculate the chain-length inequivalence (ΔC) of the different PCs, the general approach of Huang and co-workers was used (Mason et al., 1981; Huang et al., 1993). For PCs with saturated *sn*-1 and *sn*-2 chains, $\Delta C = |n_1 - n_2 + 1.5|$, where n_1 is the number of carbons in the *sn*-1 chain and n_2 is the total number of carbon atoms in the *sn*-2 acyl chain. The constant value of 1.5 accounts for a positional inequivalence of carbon atoms in the two hydrocarbon chains that occurs because the initial segment of the *sn*-2 chain extends nearly orthogonally from the *sn*-1 chain, but then bends after the second carbon atom to become roughly parallel to the *sn*-1 chain (Pearson and Pascher, 1979). In the gel phase of glycerol-based phospholipids, the end result is an axial displacement of the carbon atom positions in each chain with respect to one another by ~1.5 carbon-carbon lengths

TABLE 1 Interfacial elastic moduli of area compressibility (experimental versus fitted values at 30 mN/m)

	C_s^{-1} (mN/m)	
PC	Exptl.*	Fitted#
18:0-8:0	85	88
18:0-10:0	85	86
18:0-12:0	90	92
di-14:0	110	118
16:0-18:1$^{\Delta 9(c)}$	123	123
18:0-18:1$^{\Delta 9(c)}$	123	122
di-18:1$^{\Delta 9(c)}$	116	120
di-22:6$^{\Delta 4,7,10,13,16,19(c)}$	94	98

*Obtained from the experimental surface pressure-versus-molecular area isotherms by using the inverse of Eq. 1 (see Materials and Methods).
#Obtained by fitting the experimental surface pressure versus molecular area isotherms by using Eq. 2 and then applying the inverse of Eq. 1 to the resulting fitted isotherms. Values for di-14:0 PC, 16:0-18:1$^{\Delta 9(c)}$ PC, di-18:1$^{\Delta 9(c)}$ PC, and di-22:6$^{\Delta 4,7,10,13,16,19(c)}$ PC also appear in Smaby et al. (1997). All values pertain to liquid-expanded conditions at 24°C.

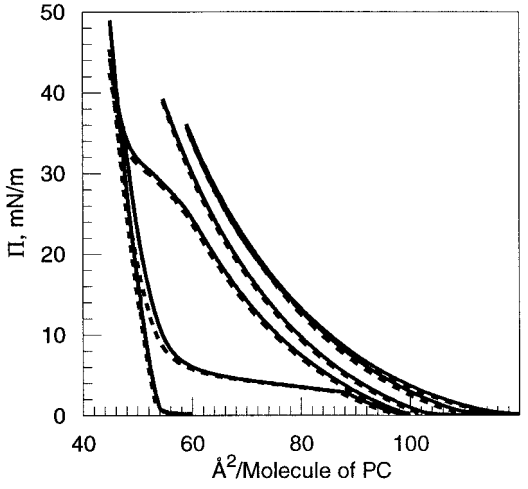

FIGURE 2 Monolayer stability of PCs with asymmetric-length acyl chains. Data were collected at 24°C on an automated Langmuir-type film balance as described in Materials and Methods. Surface pressure versus cross-sectional molecular area isotherms obtained upon compression are shown as solid lines, and those obtained upon expansion are shown as dashed lines. Barrier speed was 4 Å^2/molecule/min. No difference was observed with barrier speeds of 2, 4, 5, or 6 Å^2/molecule/min (data not shown). Isotherms (from left to right) represent PC containing a stearoyl (18:0) *sn*-1 chain and a *sn*-2 chain of 18:0, 16:0, 14:0, 12:0, 10:0, or 8:0.

(Zaccai et al., 1979). In the present study, in which the *sn*-1 chain is always stearate (18:0), the overall nonpolar chain length (*CL*) is equivalent to the number of carbon-carbon bonds in the *sn*-1 chain. From these values, the $\Delta C/CL$ ratios were calculated for the various PCs.

RESULTS

Stability of 18:0–10:0 PC monolayers

Because of the possibility that PCs with short *sn*-2 acyl chains might form unstable monolayer films, we first investigated the stability of 18:0–10:0 PC films. Fig. 1 *A* shows the surface pressure versus molecular area (π-*A*) behavior of 18:0–10:0 PC at 24°C. Classic liquid-expanded (i.e., liquid-crystalline) behavior is observed. Subsequent compression and expansion cycles, performed at different fixed barrier rates (Fig. 2), produced no significant hysteresis. This finding suggests that 18:0–10:0 PC monolayers are stable, and little if any lipid is lost from the interface during the experimental time course.

π-*A* behavior of 18:0–10:0 PC versus di-14:0 PC

To determine whether marked asymmetry in the hydrocarbon chain length of PC produces measurable effects on the force-area isotherms, the behavior of 18:0–10:0 PC was compared with that of di-14:0 PC. Although these two PCs have an identical number of total carbons in their acyl chains, the *sn*-1 chain of 18:0–10:0 PC is almost twice as long as its *sn*-2 chain when their conformational differences and their carbon numbers are taken into account (Mason et al., 1981). Using the formalism developed by Huang and colleagues, the $\Delta C/CL$ ratio of 18:0–10:0 PC equals 0.56, whereas that of di-14:0 PC equals 0.12 (see Materials and Methods). Fig. 1 *A* illustrates how the liquid-expanded behavior of 18:0–10:0 PC compares with that of di-14:0 PC at 24°C. Interestingly, the average molecular area of the 18:0–10:0 PC is ~9 Å^2 per molecule larger than that of di-14:0 PC at 1 mN/m and ~4 Å^2 per molecule larger at 30 mN/m. In fact, with respect to π-*A* behavior, the 18:0–10:0 PC behaved more like 16:0–18:1 PC than di-14:0 PC (Smaby et al., 1997).

Comparative effects of temperature on π-*A* behavior of 18:0–10:0 PC and di-14:0 PC

To investigate further how chain-length asymmetry affects the interfacial behavior of 18:0–10:0 PC compared to di-14:0 PC, the effect of temperature on the π-*A* behavior was investigated. Fig. 3 *A* shows that 18:0–10:0 PC remains liquid-expanded at various fixed temperatures between 10°C and 30°C. In contrast, di-14:0 PC is liquid-expanded at 24°C and 30°C, but isotherms measured at 20°C, 15°C, or 10°C show a two-dimensional phase transition consistent with conversion from the liquid-expanded to the liquid-condensed state (Fig. 4 *A*). The onset pressure of the phase transition decreases as the temperature is lowered. This behavior suggests that the chain-length asymmetry of 18:0–

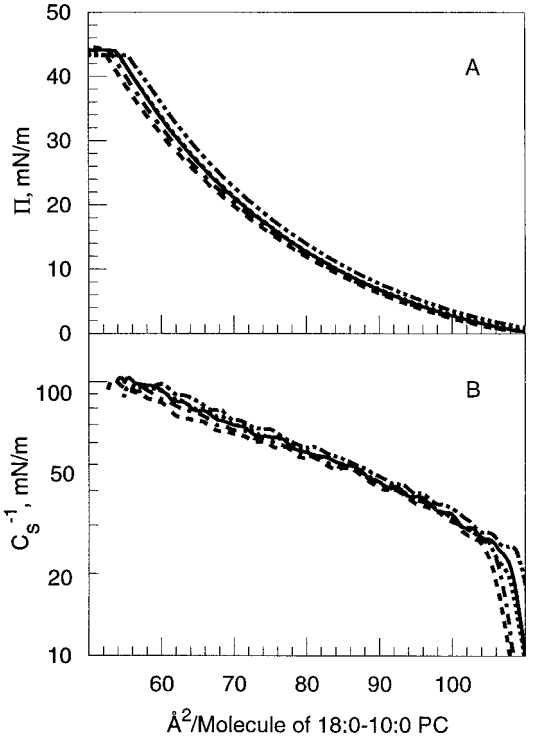

FIGURE 3 18:0–10:0 PC monolayers at different fixed temperatures. Data were collected on an automated Langmuir-type film balance (see Materials and Methods). – – –, Traces at 10°C; – · –, at 15°C; ——, at 20°C; ·····, at 24°C; – ·· –, at 30°C. (*A*) Surface pressure versus average cross-sectional molecular area (π-*A*). (*B*) Interfacial elastic modulus of area compressibility (C_s^{-1}) versus average molecular area.

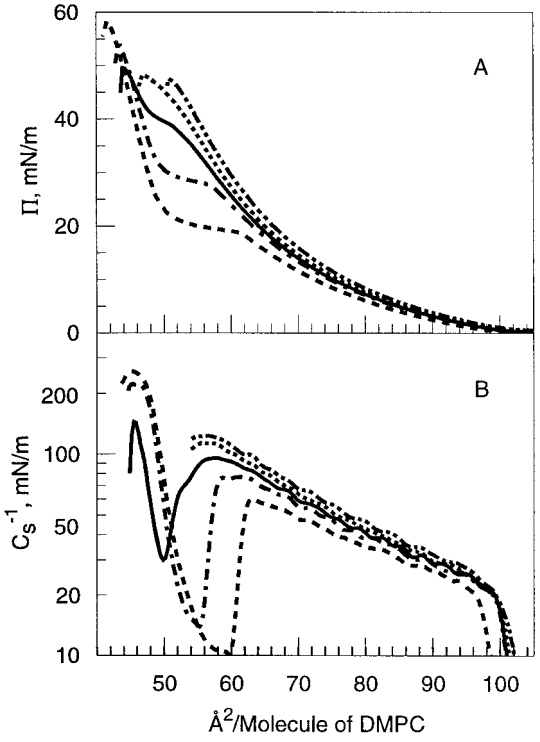

FIGURE 4 Di-14:0 PC monolayers at different fixed temperatures. (*A*) Surface pressure versus average cross-sectional molecular area (π-*A*). (*B*) Interfacial elastic modulus of area compressibility (C_s^{-1}) versus average molecular area. Other details are the same as in the legend to Fig. 3.

10:0 PC weakens the intermolecular van der Waals attractive forces and leads to a fluid phase with physical characteristics somewhat different from those of di-14:0 PC.

In-plane elasticity of 18:0–10:0 PC and di-14:0 PC monolayers

If the observed monolayer features of 18:0–10:0 PC and di-14:0 PC reflect significant differences in the physical characteristics of their liquid-expanded phases, then the average, in-plane, intermolecular elastic interactions, as indicated by the interfacial moduli of the area compressibility (C_s^{-1}), should reveal such differences. Figs. 3 *B* and 4 *B* show how the C_s^{-1} values of 18:0–10:0 PC and di-14:0 PC respond to changing cross-sectional molecular area at different fixed temperatures. Interestingly, temperature changes in the 10°C to 30°C range had very little impact on the C_s^{-1} versus area behavior of 18:0–10:0 PC (Fig. 3 *B*). The slope of the ln C_s^{-1}-versus-area plot yielded a linear response that increased ~1.33–1.35 mN/m for each square angstrom reduction in molecular cross-sectional area. The situation with di-14:0 PC markedly contrasted with that of 18:0–10:0 PC (Fig. 4 *B*). At temperatures where the isotherms showed two-dimensional phase transitions (e.g., 20°C, 15°C, and 10°C), dramatic drops in the C_s^{-1} values were observed across the phase transition region of di-14:0 PC. As pointed out previously (Smaby et al., 1996), the drop in the C_s^{-1} values upon entering the transition region most likely reflects the discontinuities in lateral packing that are known to occur when liquid-expanded and liquid-condensed phases coexist (Phillips et al., 1975; Nagle and Scott, 1978; Mouritsen et al., 1989). Upon completion of the two-dimensional transition, much higher C_s^{-1} values characteristic of liquid-condensed (i.e., gel phase) behavior were observed.

Interestingly, at membrane-like surface pressures (e.g., 30 mN/m), the C_s^{-1} value for fluid-phase 18:0–10:0 PC was 85–90 mN/m, and that of di-14:0 PC was 110–114 mN/m. Hence 18:0–10:0 PC is 20–25% more elastic in an in-plane sense than di-14:0 PC (at 30 mN/m). These differences were evident not only at 24°C but also at 30°C, temperatures where the two-dimensional transition of di-14:0 did not have an impact on the C_s^{-1} values.

Other PCs with substantial chain-length asymmetry ($\Delta C/CL \geq 0.44$)

To assess further the extent to which chain-length asymmetry influences the interfacial properties of PC, additional studies were performed with 18:0–8:0 PC and 18:0–12:0 PC. The chain-length asymmetry, as reflected in their $\Delta C/CL$ ratios, were calculated to be 0.68 for 18:0–8:0 PC and 0.44 for 18:0–12:0 PC, using the formalism developed by Huang and colleagues (see Materials and Methods). The π-*A* isotherms of these two PC derivatives obtained at various fixed temperatures are shown in Figs. 5 *A* and 6 *A*. The effect of temperature on the two-dimensional phase behavior of the lipids is evident in the isotherms. At fixed temperatures between 10°C and 30°C, 18:0–8:0 PC displayed only liquid-expanded (i.e., liquid-crystalline) behavior (Fig. 5 *A*). A similar response was noted for 18:0–12:0 PC at 15°C, 20°C, 24°C, and 30°C, but not at 10°C (Fig. 6 *A*). At this latter temperature, there was a two-dimensional phase transition after compression to 28 mN/m and 64 Å^2 per molecule.

Although 18:0–8:0 PC, 18:0–10:0 PC, and 18:0–12:0 PC exhibited liquid-expanded isotherms in the 10°C to 30°C range (exception: 18:0–12:0 PC at 10°C), subtle differences were evident. For each PC, higher temperatures resulted in slightly larger collapse areas at lower surface pressures than did reduced temperatures (Figs. 5 *A*, 3 *A*, and 6 *A*). In contrast, as the *sn*-2 chain length increased, film collapse occurred at progressively smaller cross-sectional molecular areas and higher surface pressures. Hence, with respect to collapse area, lowering the temperature by ~15°C was equivalent to increasing the *sn*-2 chain by two methylene units in terms of stabilizing the films. Moreover, the longer the *sn*-2 chain, the smaller were the "lift-off" areas (e.g., at $\pi = 1$ mN/m) for a given 1-stearoyl PC species.

Despite the subtle temperature-induced shifts in the π-*A* collapse and "lift-off" areas, analysis of the C_s^{-1} versus molecular area behavior of 18:0–8:0 PC (Fig. 5 *B*) and 18:0–12:0 PC (Fig. 6 *B*; exception: 10°C isotherm) revealed

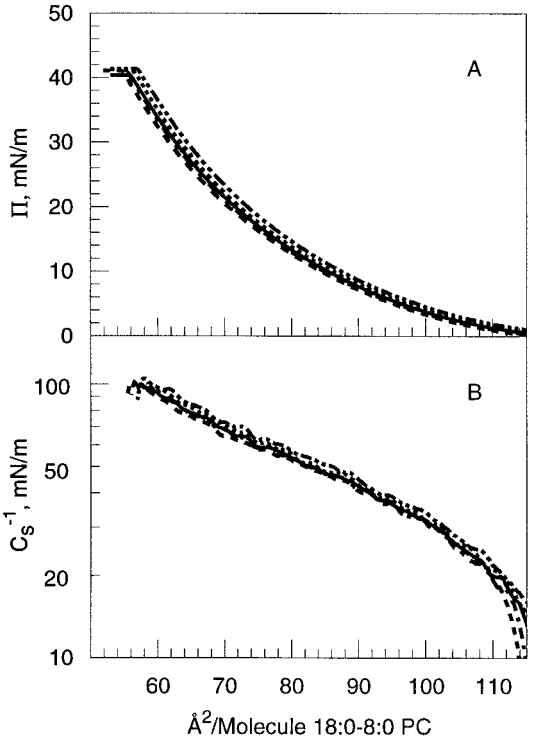

FIGURE 5 18:0–8:0 PC monolayers at different fixed temperatures. (*A*) Surface pressure versus average cross-sectional molecular area (π-*A*). (*B*) Interfacial elastic modulus of area compressibility (C_s^{-1}) versus average molecular area. Other details are the same as in the legend to Fig. 3.

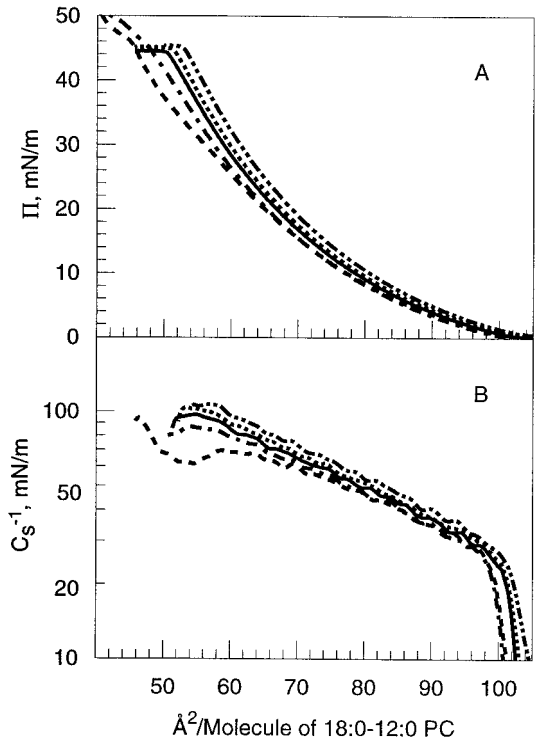

FIGURE 6 18:0–12:0 PC monolayers at different fixed temperatures. (*A*) Surface pressure versus average cross-sectional molecular area (π-*A*). (*B*) Interfacial elastic modulus of area compressibility (C_s^{-1}) versus average molecular area. Other details are the same as in the legend to Fig. 3.

that changes in temperature (10°C to 30°C range) had very little impact on interfacial elasticity. The behavior of 18:0–8:0 PC was very similar to that of 18:0–10:0 PC, in that any fixed temperature in the 10°C to 30°C range yielded a linear logarithmic response in the C_s^{-1}-versus-area plot with an increase in C_s^{-1} of ~1.33–1.35 mN/m for each square angstrom reduction in molecular cross-sectional area. Similar behavior was noted with liquid-expanded 18:0–12:0 PC, except that the linear logarithmic response in the C_s^{-1}-versus-area plot yielded an increase in C_s^{-1} of ~1.48–1.5 mN/m for each square angstrom reduction in molecular cross-sectional area. The net result was that similar interfacial elastic interactions occur (C_s^{-1} = 85–90 mN/m) for 18:0–8;0 PC, 18:0–10:0 PC, and 18:0–12:0 PC (exception: 10°C) at the membrane-like surface pressure of 30 mN/m.

It should be noted that expansion of the 18:0–8:0 PC and 18:0–12:0 PC films after compression at 24°C showed no significant hysteresis (Fig. 2). As with 18:0–10:0 PC, this finding suggests that the monolayers are stable, and little if any lipid is lost from the interface during the time course of the experiments.

PCs with moderate chain-length asymmetry ($\Delta C/CL \leq 0.32$)

Further increases in the length of the *sn*-2 chain altered the $\Delta C/CL$ ratios (e.g., 18:0–14:0 PC = 0.32 and 18:0–16:0 PC = 0.21) and resulted in films that displayed two-dimensional phase transitions of a liquid-expanded to liquid-condensed nature at many of the temperatures in the 10°C to 30°C range (Figs. 7 *A* and 8 *A*). Not surprisingly, the lower the temperature, the lower the surface pressure (and the larger the molecular area) that was observed at the onset of a two-dimensional phase transition. In contrast, di-18:0 PC, which was included for reference, displayed only liquid-condensed behavior in the 10°C to 30°C range (Fig. 9 *A*). The di-18:0 PC result agrees well with previous reports (Phillips and Chapman, 1968; Demel et al., 1972).

To determine whether moderate acyl chain-length asymmetry affects the interfacial elastic packing interactions of the PCs and to assess further the transition behavior of these moderately asymmetrical PCs, we determined their in-plane elastic interactions. The part *B* of Figs. 7–9 show how the C_s^{-1} values change as a function of molecular area for 18:0–14:0 PC, 18:0–16:0 PC, and di-18:0 PC. As noted with di-14:0 PC (Fig. 4), dramatic drops in the C_s^{-1} values are observed across the phase transition region of 18:0–14:0 PC and 18:0–16:0 PC at temperatures in the 10°C to 30°C range. Upon completion of the two-dimensional transition, higher C_s^{-1} values consistent with liquid-condensed (i.e., gel phase) behavior are observed. Unfortunately, the phase states of 18:0–14:0 PC and 18:0–16:0 PC are not exclusively liquid-crystalline at 30 mN/m and at temperatures in the 10°C to 30°C range. As a result, the 30 mN/m C_s^{-1}

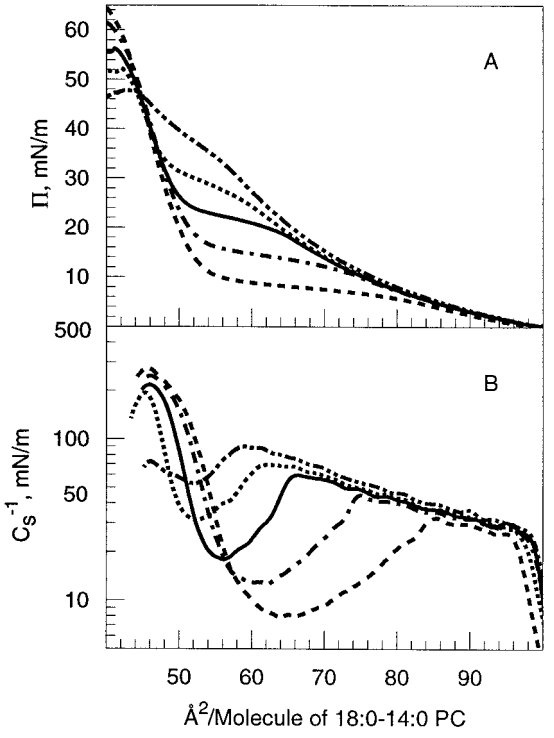

FIGURE 7 18:0–14:0 PC monolayers at different fixed temperatures. (*A*) Surface pressure versus average cross-sectional molecular area (π-*A*). (*B*) Interfacial elastic modulus of area compressibility (C_s^{-1}) versus average molecular area. Other details are the same as in the legend to Fig. 3.

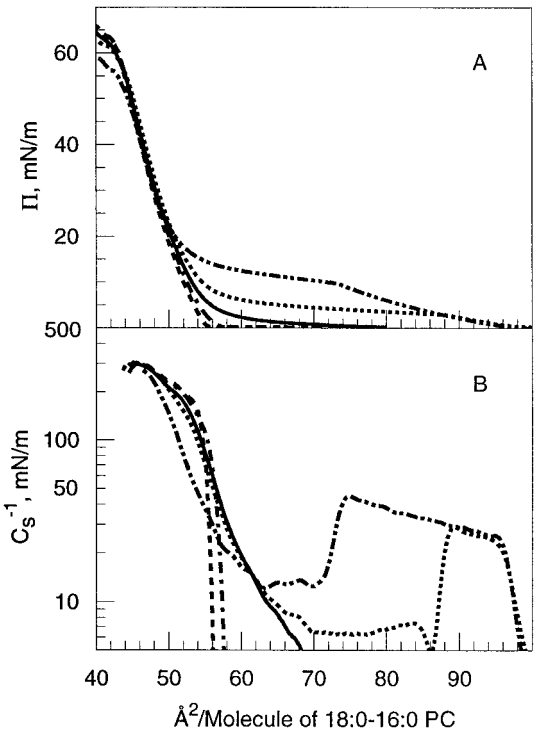

FIGURE 8 18:0–16:0 PC monolayers at different fixed temperatures. (*A*) Surface pressure versus average cross-sectional molecular area (π-*A*). (*B*) Interfacial elastic modulus of area compressibility (C_s^{-1}) versus average molecular area. Other details are the same as in the legend to Fig. 3.

values are influenced by the phase transition region and are not comparable to the 30 mN/m, fluid-phase C_s^{-1} values of 18:0–8:0 PC, 18:0–10:0 PC, 18:0–12:0 PC, and di-14:0 PC.

Expansion of the 18:0–14:0:0 PC and 18:0–16:0 PC films after compression at 24°C showed no significant hysteresis (Fig. 2). As with 18:0–10:0 PC, this finding suggests that the monolayers are stable, and little if any lipid is lost from the interface during the time course of the experiments.

DISCUSSION

Previous studies of aqueous dispersions of PCs containing saturated acyl chains of asymmetrical length have revealed that transbilayer interdigitation of the aliphatic chains is the norm when the lipids are in the gel or crystalline phase and when the hydrocarbon chains are saturated. However, the effect of chain-length asymmetry on the physical properties of fluid-phase lipids is much less clear. Under these latter conditions, aliphatic chain interdigitation is thought to be minimal or of a nonstatic nature (see Introduction). Here we have utilized Langmuir film balance approaches to investigate a PC series with a *sn*-1 chain consisting of stearate (18:0) and a *sn*-2 chain of variable length (e.g., 8:0, 10:0, 12:0, 14:0, 16:0, or 18:0). Because of their monolayer organizational arrangement, the interfacial packing interactions of many of these PCs could be studied under fluid-phase conditions, where no interdigitation was possible. However, rather than relying solely on the π-*A* behavior of the PCs, we evaluated the in-plane elasticity of the different PC films by determining their elastic moduli of area compressibility (e.g., Smaby et al., 1996, 1997).

Earlier monolayer studies involving pure PCs with asymmetrical-length acyl chains focused exclusively on π-*A* behavior. Evans et al. (1987) characterized the π-*A* behavior (at 22°C) of a series of PC species in which the *sn*-1 chains were palmitate (16:0) while the *sn*-2 chains were systematically varied (e.g., 10:0, 12:0, 14:0, 16:0, 18:0, 20:0, or 22:0). They reported liquid-expanded behavior in the PCs with saturated *sn*-2 chains of 10:0 or of 12:0 as well as the presence of a two-dimensional phase transition when the saturated *sn*-2 chain was 14:0, 16:0, or 18:0. Their results are consistent with our findings, considering the slight difference in the *sn*-1 chains (16:0 versus 18:0).

In another earlier study, Demel et al. (1967) reported that 18:0–12:0 PC at 22°C exhibited liquid-expanded π-*A* behavior that was similar to that of 18:0–18:1$^{\Delta 9(c)}$ PC. Our 18:0–12:0 PC also showed liquid-expanded behavior (at 24°C) that matched well with the π-*A* behavior of Demel et al. (1967). However, we found the shapes of the π-*A* isotherms of our 18:0–12:0 PC as well as 18:0–10:0 PC to differ from those of either 18:0–18:1$^{\Delta 9(c)}$ PC or 16:0–18:1$^{\Delta 9(c)}$ PC at surface pressures greater than 15 mN/m (Fig. 10 *A*). As a result, significant differences in their elastic moduli of area compressibility were evident at high mem-

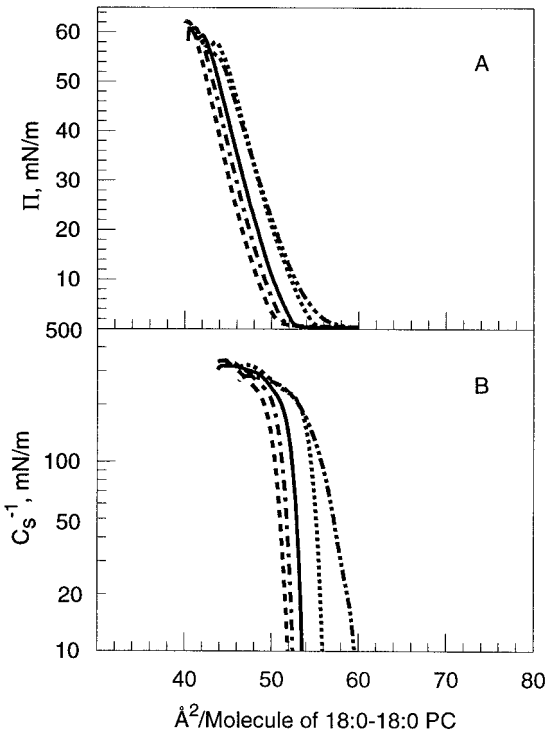

FIGURE 9 Di-18:0 PC monolayers at different fixed temperatures. (*A*) Surface pressure versus average cross-sectional molecular area (π-*A*). (*B*) Interfacial elastic modulus of area compressibility (C_s^{-1}) versus average molecular area. Other details are the same as in the legend to Fig. 3.

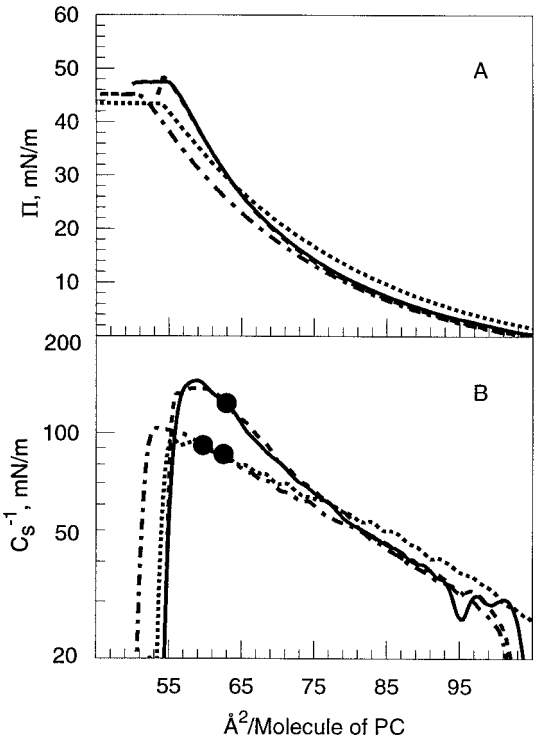

FIGURE 10 Monolayer behavior of *sn*-1 saturated PCs with either short saturated *sn*-2 chains or long unsaturated *sn*-2 chains. (*A*) Surface pressure versus average cross-sectional molecular area (π-*A*) at 24°C. – – –, 16:0–18:1$^{\Delta 9(c)}$ PC; ——, 18:0–18:1$^{\Delta 9(c)}$ PC; – · –, 18:0–12:0 PC; ·····, 18:0–10:0 PC. (*B*) Interfacial elastic modulus of area compressibility versus average molecular area (C_s^{-1}-*A*). C_s^{-1} values were calculated from the experimentally observed π-*A* isotherms in *A*, using the inverse of Eq. 1 as described in Materials and Methods. The symbol along each curve represents the surface pressure of 30 mN/m. Other details are the same as in the legend to Fig. 3.

brane-like surface pressures (Fig. 10 *B*). This is not the first time that structural alterations of the acyl chains of membrane lipids have been reported to change the in-plane elastic interactions of fluid-phase lipid assemblies. For instance, changing the number and position of *cis* double bonds in the acyl chains also is known to cause subtle but reproducible changes in the in-plane elasticity and compressibility of bilayers (e.g., Evans and Needham, 1987; Needham and Nunn, 1990; Needham, 1995; Beney et al., 1997) and of monolayers (e.g., Smaby et al., 1996, 1997). However, we are unaware of similar measurements involving bilayers composed of asymmetrical-length PCs. McIntosh et al. (1992) utilized the micropipette aspiration approach to measure the lateral area dilation moduli of bilayers composed of mixtures of equimolar cholesterol and PCs with saturated, asymmetrical-length acyl chains. No significant difference was noted in the response of asymmetrical- and symmetrical-chain-length PCs to the cholesterol. Yet, no data for the pure PCs with asymmetrical-length chains were reported.

Based on analysis of the interfacial elastic moduli of area compressibility, we find that, in the absence of acyl chain interdigitation, the in-plane elastic interactions that occur among fluid-phase PCs with markedly asymmetrical-length acyl chains differ significantly from those of fluid-phase PCs with acyl chains of approximately symmetrical length. Our goal was to focus on the in-plane elasticity of the PCs under membrane-like conditions. However, uncertainty exists as to the monolayer surface pressure value that places monolayers in equilibrium with bilayers. Many data suggest that monolayer surface pressures near 30 mN/m approximate biomembrane conditions (Marsh, 1996). Yet equally compelling evidence indicates that monolayer collapse pressures (generally >40 mN/m) reflect the equilibrium point of monolayers and bilayers (MacDonald, 1996). We arbitrarily used 30 mN/m to compare the C_s^{-1} values of the PCs investigated here (Table 2). The same relative pattern of change is observed at monolayer collapse pressures, although the magnitudes of the C_s^{-1} values increase. At 30 mN/m, the in-plane elasticity of asymmetrical chain-length PCs (e.g., 18:0–8:0 PC, 18:0–10:0 PC, or 18:0–12:0 PC) is 25% greater than that of typical fluid-phase PCs with saturated *sn*-1 chains and unsaturated *sn*-2 chains, such as 16:0–18:1$^{\Delta 9(c)}$ PC or 16:0–18:2$^{\Delta 9,12(c)}$ PC, which have C_s^{-1} values of 123 mN/m and 121 mN/m, respectively (Smaby et al., 1996, 1997). In fact, only when both acyl chains are markedly unsaturated with *cis* double bonds distributed over the entire chain length (e.g., di-22:6 PC = 94 mN/m) do the C_s^{-1} values approach those of the PCs with asymmetrical chain lengths (Smaby et al., 1997).

TABLE 2 Lipid interfacial elastic moduli of area compressibility at surface pressures of 30 mN/m

PC species	Temp. (°C)	Phase state*	Molecular area (Å^2)	C_s^{-1} (mN/m)#	PC species	Temp. (°C)	Phase state*	Molecular area (Å^2)	C_s^{-1} (mN/m)#
18:0-8:0 PC	10	L	61.7	85	18:0-16:0 PC	10	C	47.8	273
	15	L	62.3	86		15	C	48.0	264
	20	L	62.7	86		20	C	48.2	256
	24	L	63.4	85		24	C	48.5	251
	30	L	64.4	85		30	M	48.0	227
18:0-10:0 PC	10	L	60.7	82	18:0-18:0 PC	10	C	45.1	328
	15	L	61.5	83		15	C	45.9	324
	20	L	62.4	84		20	C	46.8	308
	24	L	62.5	85		24	C	48.4	306
	30	L	63.9	87		30	M	48.5	269
18:0-12:0 PC	10	M	56.0	64	14:0-14:0 PC	10	C	47.7	205
	15	L	57.4	84		15	M	50.6	39
	20	L	58.9	90		20	M	57.4	95
	24	L	59.8	90		24	L	58.5	109
	30	L	61.3	93		30	L	59.8	111
18:0-14:0 PC	10	C	47.7	230					
	15	C	48.3	211					
	20	M	48.4	135					
	24	M	53.1	36					
	30	L	60.9	90					

*Phase state: L denotes liquid-expanded (chain-disordered); C denotes condensed (chain-ordered); M denotes mixture of liquid-expanded and condensed states.

#Exptl. values calculated using the inverse of Eq. 1.

The increased in-plane elasticity observed in the fluid-phase films composed of PCs with asymmetrical-length PCs can be rationalized by considering the structural features of these molecules. First, reducing the acyl chain length of the *sn*-2 chain will effectively reduce the total van der Waals surface contacts among adjacent hydrocarbon chains. On average, the long *sn*-1 chains will have more distorted (and perhaps fewer) contacts with surrounding hydrocarbon surfaces because of the shorter *sn*-2 chains. At distances beyond the terminal methyl group of the *sn*-2 chain, the *sn*-1 chain will encounter additional voids because of the 50% drop in the average acyl chain packing density. This may encourage the distal regions of the disordered *sn*-1 chains to bend or fold back, so as to nestle into a hydrocarbon milieu rather than simply waving in the available air space. The bending and folding of the distal ends of the *sn*-1 chains back into the hydrocarbon milieu might lead to the creation of new transient voids. Second, the terminal methyl groups of the acyl chains will interfere with the attractive van der Waals packing interactions due to the larger effective volume of the terminal methyl group (e.g., 50% larger) compared to that of the methylene groups (Reiss-Husson and Luzzati, 1964; Flory, 1969). With a short *sn*-2 chain, the terminal methyl group will be located closer to the air/water interface and nearer to the middle portion of the *sn*-1 hydrocarbon chain.

The net effect of the preceding acyl chain behavior would be a weakening of intermolecular lateral interactions. Comparing the surface behavior of 18:0–10:0 PC with that of di-14:0 PC serves as a case in point. Despite the fact that these two lipids have identical numbers of total carbons in their two acyl chains, the π-A isotherms at 24°C show that 18:0–10:0 PC is between 4 and 9 Å^2 per molecule larger than di-14:0 PC (depending on surface pressure), despite the fact that they both display liquid-expanded behavior. Moreover, lowering the temperature to 20°C, 15°C, or 10°C has almost no effect on 18:0–10:0 PC, but induces two-dimensional phase transitions in the π-A isotherms of di-14:0 PC. Finally, analyzing the in-plane elasticity of the 18:0–10:0 PC films at 30 mN/m at both 24°C and 30°C reveals experimental C_s^{-1} values of 91 mN/m at both temperatures, whereas those of di-14:0 PC films are 110 mN/m. Hence all of the preceding observations are consistent with a weakening of the intermolecular attractive forces in the 18:0–10:0 PC monolayers relative to di-14:0 PC monolayers.

As was pointed out in the Introduction, previous Fourier transform infrared, fluorescence, and diffraction studies of liquid-crystalline bilayers composed of PCs with highly asymmetrical chain lengths suggest that a "statistical" sort of partial transbilayer interdigitation occurs, with the longer acyl chains rapidly sampling both their own as well as the apposing monolayer (Lewis et al., 1994; Mason, 1994; Zhu and Caffrey, 1993). Indeed, x-ray diffraction studies indicate that the liquid-crystalline bilayer thickness of 18:0–10:0 PC is consistent with significant overlap of the acyl chains from apposing monolayers (McIntosh et al., 1984; Zhu and Caffrey, 1993). Magic-angle spinning NMR approaches of liquid-crystalline 18:0–10:0 PC suggest motionally restricted acyl chains (based on segmental reorientation at megahertz frequencies), but enhanced chain or bilayer motions based on rotating-frame relaxation times at midkilohertz frequencies (Halladay et al., 1990). Fluorescence studies involving anthroyloxy derivatives of fatty acids in bilayers of PCs with saturated asymmetrical-length

acyl chains have revealed how the order parameter changes in response to fluorescent probe depth. A characteristic "interdigitation signature" response of the anisotropy order profile has been noted that is distinct from that of PCs with symmetrical-length acyl chains. Mason (1994) attributed the unique anisotropy profiles of the liquid-crystalline phase of the PCs containing chain-length asymmetry to a transient interpenetration of the chains from the opposing leaflets of the bilayer. Moreover, recent analyses of the molecular geometry of liquid-crystalline 18:0–10:0 PC based on the "shape factor" developed by Israelachvili (1992) reveal a value that is very near the transition from a nonspherical micellar to a bilayer vesicle morphology (Mason et al., 1995).

Taken together, the preceding studies indicate that the physical environment of liquid-crystalline bilayers is altered by chain-length asymmetry in membrane lipids. However, in contrast to the earlier bilayer studies in which the observed change in membrane properties were attributed solely to transient "statistical" interdigitation of the acyl chains, the monolayer data reported here reveal other differences in the ways that PCs with asymmetrical chain lengths interact with one another. We find fundamental differences in the in-plane elasticity of such PCs under conditions where acyl chain interdigitation cannot be a contributing factor. Admittedly, the applicability of the monolayer situation to that of the bilayer must be viewed with caution, given that the energy barrier for extension of the distal portions of the *sn*-1 chains into apposing hydrocarbon chains in bilayers is likely to be lower than that encountered in monolayers. Nonetheless, the monolayer results provide interesting possibilities to consider regarding an earlier translational diffusion study in which the lateral diffusion rate of NBD-labeled PE was compared in liquid-crystalline 18:0–10:0 PC and in di-14:0 PC bilayers. In that study, Schram and Thompson (1995) postulated that liquid-crystalline PCs with asymmetrical-length acyl chains would be expected to encounter a frictional drag along the bilayer midplane due to transient "statistical" interdigitation of the acyl chains. However, their translational diffusion measurements revealed no significant differences in the NBD-PE movement within fluid-phase 18:0–10:0 PC and di-14:0 PC. If the in-plane elasticity of 18:0–10:0 PC exceeds that of di-14:0 PC in bilayers, as is the case in monolayers, the expected frictional drag along the bilayer midplane of 18:0–10:0 PC might be offset in some manner by its higher in-plane elasticity. Obviously, further experiments will be needed to test this interpretation.

The preceding discussion illustrates how hydrocarbon chain-length asymmetry in membrane lipids may play an important role in modulating the physical features of liquid-crystalline bilayers. Although PCs with acyl chain-length asymmetry may be of minor consequence in mammalian cells, these lipids are readily produced within the membranes of simple eukaryotes subjected to conditions of environmental and/or nutritional stress (Meyer and Bloch, 1963; Proudlock et al., 1971). In mammalian systems, however, other lipid types, such as sphingolipids, are known to possess marked asymmetry in their hydrocarbon regions under normal physiological conditions. The impact of the hydrocarbon chain-length asymmetry in sphingolipids is an area of growing interest in cell membrane biophysics.

This investigation was supported by U.S. Public Health Service grant GM45928 (REB) and the Hormel Foundation. The automated Langmuir film balance used in this investigation received major support from U.S. Public Health Service grants HL49180 and HL17371 (HLB). We also thank the anonymous referees for their helpful insights.

REFERENCES

Ali, S., and R. Bittman. 1989. Mixed-chain phosphatidylcholine analogues modified in the choline moiety: preparation of isomerically pure phospholipids with bulky head groups and one acyl chain twice as long as the other. *Chem. Phys. Lipids.* 50:11–21.

Ali, S., H. L. Brockman, and R. E. Brown. 1991. Structural determinants of miscibility in surface films of galactosylceramide and phosphatidylcholine: effect of unsaturation in the galactosylceramide acyl chain. *Biochemistry.* 30:11198–11205.

Ali, S., J. M. Smaby, H. L. Brockman, and R. E. Brown. 1996. Phosphatidylcholines with saturated, asymmetric-length acyl chains: a Langmuir film balance investigation. *Biophys. J.* 70:A88.

Bartlett, G. R. 1959. Phosphorus assay in column chromatography. *J. Biol. Chem.* 234:466–468.

Behroozi, F. 1996. Theory of elasticity in two dimensions and its application to Langmuir-Blodgett films. *Langmuir.* 12:2289–2291.

Beney, L., J.-M. Perrier-Cornet, M. Hayert, and P. Gervais. 1997. Shape modification of phospholipid vesicles induced by high pressure: influence of bilayer compressibility. *Biophys. J.* 72:1258–1263.

Davies, J. T., and E. K. Rideal. 1963. Interfacial Phenomena, 2nd Ed. Academic Press, New York. 265.

Demel, R. A., W. S. M. Geurts van Kessel, and L. L. M. van Deenen. 1972. The properties of polyunsaturated lecithins in monolayers and liposomes and the interactions of these lecithins with cholesterol. *Biochim. Biophys. Acta.* 266:26–40.

Demel, R. A., L. L. M. van Deenen, and B. A. Pethica. 1967. Monolayer interactions of phospholipids and cholesterol. *Biochim. Biophys. Acta.* 135:11–19.

Evans, E., and D. Needham. 1987. Physical properties of surfactant bilayer membranes: thermal transitions, elasticity, rigidity, cohesion, and colloidal interactions. *J. Phys. Chem.* 91:4219–4228.

Evans, R. W., M. A. Williams, and J. Tinoco. 1987. Surface areas of 1-palmitoyl phosphatidylcholines and their interactions with cholesterol. *Biochem. J.* 245:455–462.

Feng, S.-S., H. L. Brockman, and R. C. MacDonald. 1994. On osmotic-type equations of state for liquid-expanded monolayers of lipids at the air-water interface. *Langmuir.* 10:3188–3194.

Flory, P. J. 1969. Statistical Mechanics of Chain Molecules. Wiley-Interscience, New York.

Halladay, H. N., R. E. Stark, S. Ali, and R. Bittman. 1990. Magic-angle spinning NMR studies of molecular organization in multibilayers formed by 1-octadecanoyl-2-decanoyl-*sn*-glycero-3-phosphocholine. *Biophys. J.* 58:1449–1461.

Huang, C. 1990. Mixed-chain phospholipids and interdigitated bilayer systems. *Klin. Wochenschr.* 68:149–165.

Huang, C., S. Li, Z. Wang, and H. Lin. 1993. Dependence of the bilayer phase transition temperatures on the structural parameters of phosphatidylcholines. *Lipids.* 28:365–370.

Huang, C., and J. T. Mason. 1986. Structure and properties of mixed-chain phospholipid assemblies. *Biochim. Biophys. Acta.* 864:423–470.

Hui, S.-W., J. T. Mason, and C. Huang. 1984. Acyl chain interdigitation in saturated mixed-chain phosphatidylcholine bilayer dispersions. *Biochemistry.* 23:5570–5577.

Israelachvili, J. 1992. Intermolecular and Surface Forces. Academic Press, New York. 366–394.

Lewis, R. N. A. H., R. N. McElhaney, M. Monck, and P. R. Cullis. 1994. Studies of highly asymmetric mixed-chain diacyl phosphatidylcholines that form mixed-interdigitated gel phases: Fourier transform infrared and ^{2}H NMR spectroscopic studies of hydrocarbon chain conformation and orientational order in the liquid-crystalline state. *Biophys. J.* 67: 197–207.

MacDonald, R. C. 1996. The relationship and interactions between lipid bilayer vesicles and lipid monolayers at the air/water interface. *In* Vesicles. M. Rosoff, editor. Marcel Dekker, New York. 3–48.

Marsh, D. 1996. Lateral pressure in membranes. *Biochim. Biophys. Acta.* 1286:183–223.

Mason, J. T. 1994. Properties of phosphatidylcholine bilayers as revealed by mixed-acyl phospholipid fluorescent probes containing *n*-(9-anthroyloxy) fatty acids. *Biochim. Biophys. Acta.* 1194:99–108.

Mason, J. T., R. E. Cunningham, and T. J. O'Leary. 1995. Lamellar-phase polymorphism in interdigitated bilayer assemblies. *Biochim. Biophys. Acta.* 1236:65–72.

Mason, J. T., C. Huang, and R. L. Biltonen. 1981. Calorimetric investigations of saturated mixed-chain phosphatidylcholine bilayer dispersions. *Biochemistry.* 20:6086–6092.

McIntosh, T. J., S. A. Simon, J. C. Ellington, and N. A. Porter. 1984. New structural model for mixed-chain phosphatidylcholine bilayers. *Biochemistry.* 23:4038–4044.

McIntosh, T. J., S. A. Simon, D. Needham, and C. Huang. 1992. Structure and cohesive properties of sphingomyelin/cholesterol bilayers. *Biochemistry.* 31:2012–2020.

Meyer, F., and K. Bloch. 1963. Metabolism of stearolic acid in yeast. *J. Biol. Chem.* 238:2654–2659.

Middleton, S. R., and B. A. Pethica. 1981. Electric field effects on monolayers at the air-water interface. *Faraday Symp. Chem. Soc.* 16:109–123.

Momsen, W. E., J. M. Smaby, and H. L. Brockman. 1990. The suitability of nichrome for measurement of gas-liquid interfacial tension by the Wilhelmy method. *J. Colloid Interface Sci.* 135:547–552.

Mouritsen, O. G., J. H. Ipsen, and M. J. Zuckermann. 1989. Lateral density fluctuations in the chain-melting phase transition of lipid monolayers. *J. Colloid Interface Sci.* 129:32–40.

Nagle, J. F., and H. L. Scott. 1978. Lateral compressibility of lipid mono- and bilayers: theory of membrane permeability. *Biochim. Biophys. Acta.* 513:236–243.

Needham, D. 1995. Cohesion and permeability of lipid bilayer vesicles. *In* Permeability and Stability of Lipid Bilayers. E. A. Disalvo and S. A. Simon, editors. CRC Press, Boca Ration, FL. 49–76.

Needham, D., and R. S. Nunn. 1990. Elastic deformation and failure of lipid bilayer membranes containing cholesterol. *Biophys. J.* 58: 997–1009.

Pearson, R. H., and I. Pascher. 1979. The molecular structure of lecithin dihydrate. *Nature.* 281:499–501.

Phillips, M. C., and D. Chapman. 1968. Monolayer characteristics of saturated 1,2-diacyl phosphatidylcholines (lecithins) and phosphatidylethanolamines at the air-water interface. *Biochim. Biophys. Acta.* 163:301–313.

Phillips, M. C., D. E. Graham, and H. Hauser. 1975. Lateral compressibility and penetration into phospholipid monolayers and bilayer membranes. *Nature.* 254:154–155.

Proudlock, J. W., J. M. Haslam, and A. W. Linnane. 1971. Biogenesis of mitochondria 19. The effects of unsaturated fatty acid depletion on the lipid composition and energy metabolism of a fatty acid desaturase mutant of *Saccharomyces cerevisiae*. *J. Bioenerg.* 2:327–349.

Reiss-Husson, F., and V. Luzzati. 1964. The structure of the micellar solutions of some amphiphilic compounds in pure water as determined by absolute small-angle X-ray scattering techniques. *J. Phys. Chem.* 68:3504–3511.

Schram, V., and T. E. Thompson. 1995. Interdigitation does not affect translational diffusion of lipids in liquid crystalline bilayers. *Biophys. J.* 69:2517–2520.

Schwarz, G., G. Wackerbauer, and S. E. Taylor. 1996. Partitioning of a nearly insoluble lipid monolayer into its aqueous subphase. *Colloids Surf.* 111:39–47.

Slater, J. L., and C. Huang. 1988. Interdigitated bilayer membranes. *Prog. Lipid Res.* 27:325–359.

Slater, J. L., and C. Huang. 1992. Lipid bilayer interdigitation. *In* The Structure of Biological Membranes. P. L. Yeagle, editor. CRC Press, Boca Raton FL. 175–210.

Smaby, J. M., and H. L. Brockman. 1990. Surface dipole moments of lipids at the argon-water interface. Similarities among glycerol-ester-based lipids. *Biophys. J.* 58:195–204.

Smaby, J. M., and H. L. Brockman. 1991a. A simple method for estimating surfactant impurities in solvents and subphases used for monolayer studies. *Chem. Phys. Lipids.* 58:249–252.

Smaby, J. M., and H. L. Brockman. 1991b. Evaluation of models for surface pressure-area behavior of liquid-expanded monolayers. *Langmuir.* 7:1031–1034.

Smaby, J. M., and H. L. Brockman. 1992. Characterization of lipid miscibility in liquid-expanded monolayers at the gas-liquid interface. *Langmuir.* 8:563–570.

Smaby, J. M., V. S. Kulkarni, M. Momsen, and R. E. Brown. 1996. The interfacial elastic packing interactions of galactosylceramides, sphingomyelins, and phosphatidylcholines. *Biophys. J.* 70:868–877.

Smaby, J. M., M. Momsen, H. L. Brockman, and R. E. Brown. 1997. Phosphatidylcholine acyl unsaturation modulates the decrease in interfacial elasticity induced by cholesterol. *Biophys. J.* 73:1492–1505.

Wolfe, D. H., and H. L. Brockman. 1988. Regulation of the surface pressure of lipid monolayers and bilayers by the activity of water: derivation and application of an equation of state. *Proc. Natl. Acad. Sci. USA.* 85:4285–4289.

Zaccai, G., G. Büldt, A. Seelig, and J. Seelig. 1979. Neutron diffraction studies on phosphatidylcholine model membranes. II. Chain conformation and segmental order. *J. Mol. Biol.* 134:693–706.

Zhu, T., and M. Caffrey. 1993. Thermodynamic, thermomechanical, and structural properties of a hydrated asymmetric phosphatidylcholine. *Biophys. J.* 65:939–954.